DOI: 10.1111/j.1467-8659.2011.02072.x

COMPUTER GRAPHICS *forum*
Volume 30 (2011), number 8 pp. 2427–2439

A General BRDF Representation Based on Tensor Decomposition

Ahmet Bilgili[1], Aydın Öztürk[2] and Murat Kurt[1]

[1]International Computer Institute, Ege University, Turkey
ahmetbilgili@gmail.com and murat.kurt@ege.edu.tr
[2]Department of Computer Engineering, Yasar University, Turkey
aydin.ozturk@yasar.edu.tr

Abstract

Generating photo-realistic images through Monte Carlo rendering requires efficient representation of light–surface interaction and techniques for importance sampling. Various models with good representation abilities have been developed but only a few of them have their importance sampling procedure. In this paper, we propose a method which provides a good bidirectional reflectance distribution function (BRDF) representation and efficient importance sampling procedure. Our method is based on representing BRDF as a function of tensor products. Four-dimensional measured BRDF tensor data are factorized using Tucker decomposition. A large data set is used for comparing the proposed BRDF model with a number of well-known BRDF models. It is shown that the underlying model provides good approximation to BRDFs.

Keywords: BRDF representation, importance sampling, global illumination, rendering, Tucker decomposition

ACM CCS: I.3.7 [Computer Graphics]: Three-Dimensional Graphics and Realism

1. Introduction

The problem of developing an adequate representation for the distribution of light scattered from a surface has been studied extensively in computer graphics. The bidirectional reflectance distribution function (BRDF) is commonly used to describe surface reflectance. A wide range of models have been proposed to approximate the BRDFs.

The incoming radiance (L_i) and outgoing radiance (L_o) are closely related through the BRDF (ρ) by the following well-known relationship:

$$L_o(\vec{\omega}_o) = \int_\Omega L_i(\vec{\omega}_i)\rho(\vec{\omega}_i, \vec{\omega}_o)(\vec{\omega}_i \cdot \mathbf{n})\, \mathrm{d}\vec{\omega}_i, \qquad (1)$$

where $\vec{\omega}_i = (\theta_i, \phi_i)$ and $\vec{\omega}_o = (\theta_o, \phi_o)$ are the incoming and outgoing direction vectors with elevation and azimuth angles θ and ϕ, respectively, and $\mathbf{n}$ is the surface normal vector.

Computing the outgoing radiance involves two important issues that need to be resolved. First we need to find an adequate model for representing the BRDF, and second we need to develop an efficient importance sampling procedure for evaluating the integral in Eq. (1) by using Monte Carlo techniques. Various models with good representation abilities have been developed but a few of them have their importance sampling procedure.

In this work, we propose to represent the BRDF by employing tensor products. Tensor products are based on factorizing the underlying data into certain components. Using different techniques, several researchers have investigated the possibility of BRDF factorization for real-time rendering [KM99, MAA01]. Lawrence et al. [LRR04] used non-negative matrix factorization (NMF) to represent BRDF as a product of univariate probability distributions. They used this factorization especially for efficient importance sampling. Our approach provides a general method for both efficient BRDF representation and simple importance sampling procedure. Empirical results show that the proposed method achieves high compression ratios *CR*s while maintaining certain properties of BRDF including Fresnel effects and off-specularity.

A physically plausible BRDF representation should dictate non-negativity, Helmholtz reciprocity and energy conservation [NNSK99, EBJ*06]. Our visually plausible representation satisfies the non-negativity property, but not the others, namely, the Helmholtz reciprocity and the energy conservation.

For representing the measured BRDF, we use Tucker decomposition algorithm. This algorithm is used for computing the tensor factors. Our BRDF model is based on halfway vector representation of the BRDF, followed by a compact and accurate decomposition of this four-dimensional (4D) representation into univariate factors. We evaluate the 4D BRDF as the sum of terms, each of which is defined as the product of four univariate functions.

The proposed method also lends itself to developing an efficient and simple importance sampling algorithm. The most significant factors are identified and selected by using Tucker's orthogonal projections, and samples are generated from the bivariate probability distributions of these factors. Extensive empirical comparisons with a number of well-known models have shown that the proposed model provides good approximation to measured BRDFs for various isotropic and anisotropic materials.

2. Previous Work

The BRDF is the core part of the rendering equation [Kaj86]. Therefore, a wide range of BRDF models have been proposed to represent surface reflectance. These models can be classified in two main groups: analytical BRDF models and data-driven BRDF models.

2.1. Analytical BRDF models

One of the most well-known analytical model, is the Phong model [Pho75]. An improved version of the Phong model [Pho75] is the Blinn–Phong model [Bli77]. While the Phong model is based on reflection vector, the Blinn–Phong model is based on halfway vector. The halfway vector-based BRDF representation is more convenient than the reflection vector-based representation [NDM05]. Ward [War92] proposed a simple formula to describe isotropic and anisotropic surface reflectance. Lafortune et al. [LFTG97] obtained a generalization of the Phong BRDF model. This generalized Phong model can represent non-Lambertian diffuse reflection, retro-reflection and the Fresnel effects. Duer [Due05] presented a variation of the Ward BRDF model, known as the Ward–Duer BRDF model. This model has a different normalization factor from the Ward representation, and thus improves the fitting results [NDM05]. The Phong, the Blinn-Phong, the Ward, the Ward-Duer and the Lafortune models are phenomenological models. Some physically based BRDF models also have been developed. The BRDF models of this category (e.g. [TS67, CT81, HTSG91, ON94]) are more sophisticated and can represent effects such as a Fresnel reflection and rough micro-geometry. Anisotropic BRDF models [Kaj85, PF90, War92, LFTG97, AS00, Due05, EBJ*06] can represent the reflective properties of oriented surfaces such as brushed metal, satin and velvet.

The aforementioned analytical BRDF models have non-linear parameters. On the other hand, the BRDF can be approximated using linear functions [WAT92, SS95, KvDS96, LF97, OKBG08]. Westin et al. [WAT92] used spherical harmonics; Koenderink et al. [KvDS96] used Zernike polynomials; Schröder and Sweldens [SS95] and Lalonde and Fournier [LF97] used wavelets; Stark et al. [SAS05] proposed a new barycentric coordinate system with respect to a triangular support for reducing the dimensionality of some BRDF models; and Öztürk et al. [OKBG08] used Principal Component (PC) transformations of some explanatory variables for approximating BRDFs linearly. The main disadvantage of these linear BRDF models is that they require a large number of coefficients to represent BRDFs accurately.

2.2. Data-driven BRDF models

Acquiring dense measurements of the BRDF and using these measurements directly in the rendering process have been used in [MPBM03]. Unfortunately, this technique has large storage complexity. Therefore, accurate and compact representations of measured BRDFs using factorization have been investigated [KM99, MAA01, LRR04]. In all cases, 4D BRDFs have been factored into product of two-dimensional (2D) functions. More importantly, only Lawrence et al. [LRR04] have developed an importance sampling procedure. For isotropic BRDFs, Romeiro et al. [RVZ08] reduced the measured BRDF data into a 2D representation by averaging BRDF around ϕ_d, which is one of the parameters defining incident vector in the Rusinkiewicz [Rus98] coordinate system.

2.3. Importance sampling

Many analytical BRDF models [Pho75, Bli77, War92, LFTG97, AS00, Due05, EBJ*06] have their own importance sampling procedures. Importance sampling algorithms are not available for some analytical BRDF models [TS67, CT81]. Some other analytical models which have importance sampling schemes, often have problems approximating more complex BRDFs. Furthermore, fitting these analytical BRDF models to measured data often is not trivial and non-linear optimizers must be used. These optimizers need careful user intervention when fitting more than two specular lobes [LRR04]. Lawrence et al. [LRR04] presented a factored BRDF model, which has an efficient importance sampling procedure. Lawrence et al. [LRR05] proposed an importance sampling algorithm which depends on polygonal approximation of multi-dimensional tabular cumulative

distribution functions (cdfs) using Douglas–Peucker algorithm. This algorithm requires large storage space but provides low variance results for BRDF sampling. This algorithm also enables importance sampling of environment maps. A sampling algorithm proposed by Montes et al. [MUGL08], is based on rejection sampling of hierarchical parameterless probability distribution functions (pdfs). Their hierarchical structure reduces the number of fails in rejection sampling, thus it increases the sampling speed and reduces the variance.

2.4. Tensor approximation using factorization

In computer graphics, tensor approximations using factorization [KB09] have been used for data compression [VT04, WWS*05]. Sun et al. [SZC*07] employed Tucker decomposition to decompose the BRDF data. They used this decomposition method to represent BRDF in a real-time global illumination algorithm. They decomposed the data into three 2D matrices and a core tensor. Following a similar decomposition method we use univariate tensor functions to estimate the BRDF recursively. Furthermore, we use Tucker decomposition to develop an efficient important sampling procedure.

Similarly we also employ Tucker decomposition to represent the measured BRDF data, but opposed to storing data as 2D matrices and core tensor we evaluate the 4D BRDF as the sum of terms, each of which is defined as the product of four univariate functions.

3. Tensors and Tucker Factorization

Tensors are geometric entities presented to generalize the notion of scalars, vectors and matrices to higher orders. The order of the tensor is defined as the number of dimensions used to represent the multi-way arrays. For example, a first-order tensor can be viewed as a vector, a second-order tensor as a matrix, a third-order tensor as a cube and so on.

The problem of expressing a tensor as a product of certain factors was first studied by Hitchcock in 1927 [Hit27a, Hit27b] but it is named after the work of Tucker [Tuc63, Tuc64, Tuc66]. Basically, the Tucker factorization is a generalization of higher order principal component analysis that decomposes a tensor into a set of matrices and one small core tensor. It has been used widely in various fields including image compression, data mining and psychometrics. A good review of the topic can be found in [KB09].

The Tucker decomposition of a three-dimensional (3D) matrix $\mathbf{T} = \{t_{ijk}\}, i = 1, \ldots, I, j = 1, \ldots, J, k = 1, \ldots, K$ into a small 3D matrix $\mathbf{G} = \{g_{pqr}\}, p = 1, \ldots, P, q = 1, \ldots, Q, r = 1, \ldots, R$ and three 2D matrices $\mathbf{X} = \{x_{ip}\}, \mathbf{Y} = \{y_{jq}\}, \mathbf{Z} = \{z_{kr}\}$, is illustrated in Figure 1 . Based on this representation, a tensor element

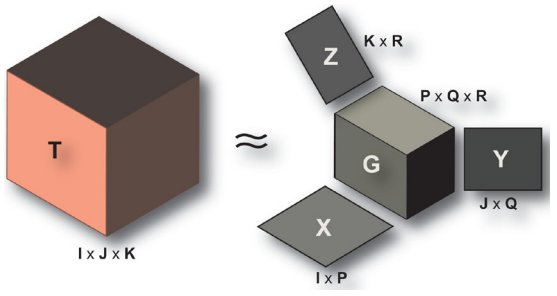

Figure 1: *Tucker factorization of a 3D tensor: Three univariate factors and a scalar constant representing the core tensor.*

t_{ijk} can be approximated by

$$t_{ijk} \approx \sum_{p=1}^{P} \sum_{q=1}^{Q} \sum_{r=1}^{R} g_{pqr} x_{ip} y_{jq} z_{kr}, \tag{2}$$

The 4D BRDF data can be represented through a Tucker representation in a similar way as explained in the above example. Our BRDF model is based on the halfway vector representation. The halfway vector $\vec{\omega}_h = (\theta_h, \phi_h)$ is defined in terms of $\vec{\omega}_i$ and $\vec{\omega}_o$ as

$$\vec{\omega}_h = \frac{\vec{\omega}_i + \vec{\omega}_o}{\|\vec{\omega}_i + \vec{\omega}_o\|}. \tag{3}$$

The halfway vector parametrization aligns certain BRDF features with directions of certain BRDF phenomena [NDM05].

Non-negativity of the estimated BRDF values is an important issue to consider in modelling BRDF data. Lawrence et al. [LRR04] have employed NMF algorithm to avoid negative BRDFs. In this paper we used the logarithmic transformation of the measured BRDF data. The logarithmic transformation not only provides a more convenient input for the Tucker factorization but also eliminates the problem of estimated negative BRDF values.

For a given 4D sample matrix $\mathbf{B} = \{b_{ijkl}\}, i = 1, \ldots, N_{\theta_h}, j = 1, \ldots, N_{\phi_h}, k = 1, \ldots, N_{\theta_o}, l = 1, \ldots, N_{\phi_o}$, where $N_{\theta_h}, N_{\phi_h}, N_{\theta_o}$ and N_{ϕ_o} are the sampling resolutions for each tensor axis, corresponding expression for the BRDF can be written as

$$b_{ijkl} \approx \sum_{p=1}^{n_{\theta_h}} \sum_{q=1}^{n_{\phi_h}} \sum_{r=1}^{n_{\theta_o}} \sum_{s=1}^{n_{\phi_o}} g_{pqrs} x_{ip} y_{jq} z_{kr} w_{ls}, \tag{4}$$

where $\mathbf{X} = \{x_{ip}\}, p = 1, \ldots, n_{\theta_h}, \mathbf{Y} = \{y_{jq}\}, q = 1, \ldots, n_{\phi_h}, \mathbf{Z} = \{z_{kr}\}, r = 1, \ldots, n_{\theta_o}$ and $\mathbf{W} = \{w_{ls}\}, s = 1, \ldots, n_{\phi_o}$ are the factor matrices and $\mathbf{G} = \{g_{pqrs}\}$ is the core tensor matrix and $n_{\theta_h}, n_{\phi_h}, n_{\theta_o}$ and n_{ϕ_o} are the Tucker parameters. When $n_{\theta_h}, n_{\phi_h}, n_{\theta_o}$ and n_{ϕ_o} are smaller than $N_{\theta_h}, N_{\phi_h}, N_{\theta_o}$ and N_{ϕ_o}, respectively, then the corresponding

core matrix **G** can be viewed as a compressed version of the BRDF matrix **B**.

4. Approximating the BRDF Using the Tucker Factorization

As is seen from Eq. (4), the Tucker factorization involves the evaluation of four nested loops, each of which requires a large number of iterations. Naturally, the accuracy of the approximation is improved at the expense of increased computational cost. For certain applications the underlying cost can be prohibitively large. On the other hand, decreasing the number of iterations would cause large approximation errors. To provide an intermediate solution to the problem, we propose first to simplify the approximation procedure by setting the parameters $n_{\theta_h}, n_{\phi_h}, n_{\theta_o}$ and n_{ϕ_o} of the Tucker factorization all to 1 in Eq. (4) and then reduce the error of approximation in a stepwise manner. From the point of practical application, it turns out that this approach not only provides a simple approximation to the BRDF but is also a good ground for importance sampling.

Based on the simplified expression $n_{\theta_h} = n_{\phi_h} = n_{\theta_o} = n_{\phi_o} = 1$, the corresponding Tucker approximation for a 4D BRDF can be expressed as

$$\log(b_{ijkl}) \approx g f_1(\theta_{hi}) f_2(\phi_{hj}) f_3(\theta_{ok}) f_4(\phi_{ol}), \tag{5}$$

where g is the core tensor which is a scalar for this simplified case; $f_1(\theta_{hi})$, $f_2(\phi_{hj})$, $f_3(\theta_{ok})$ and $f_4(\phi_{ol})$ are univariate tensor functions evaluated at θ_{hi}, ϕ_{hj}, θ_{ok} and ϕ_{ol}; and $i = 1, \ldots, N_{\theta_h}$, $j = 1, \ldots, N_{\phi_h}$, $k = 1, \ldots, N_{\theta_o}$ and $l = 1, \ldots, N_{\phi_o}$ are the 4D BRDF matrix indices.

Clearly, Eq. (5) provides a rough approximation to the BRDF. To improve the accuracy of this approximation we propose applying the Tucker factorization recursively on the corresponding error term. The first approximation model in Eq. (5) can be rewritten as

$$\mathbf{B}_0 = \mathbf{B}'_0 + \mathbf{e}_1, \tag{6}$$

where $\mathbf{B}_0$ is the data matrix based on logarithms of the BRDFs; $\mathbf{B}'_0$ is the approximation to $\mathbf{B}_0$; and $\mathbf{e}_1$ is the error matrix of this first approximation. Next we model the error term in a similar way as

$$\mathbf{e}_1 = \mathbf{e}'_1 + \mathbf{e}_2, \tag{7}$$

where $\mathbf{e}'_1$ is the Tucker approximation of $\mathbf{e}_1$, and $\mathbf{e}_2$ is the error term of the second approximation. This process is continued until a satisfactory level of accuracy is obtained. Finally, the log BRDF values can be approximated by

$$\mathbf{B}_0 \approx \mathbf{B}'_0 + \mathbf{e}'_1 + \mathbf{e}'_2 + \cdots + \mathbf{e}'_{L-1}, \tag{8}$$

where L is the total number of iterations. Accuracy of the approximation closely depends on the number of iterations and needs to be determined empirically. This process is illustrated in Figure 2 .

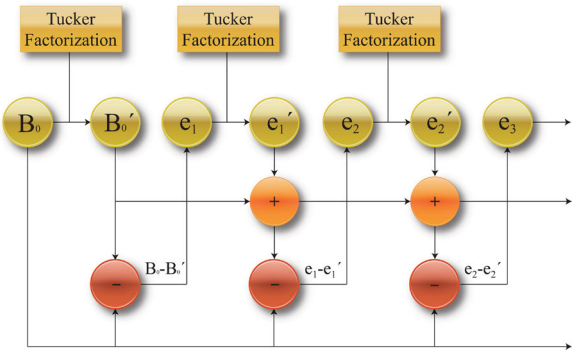

Figure 2: *This figure shows error modelling using Tucker factorization. In this figure,* $\mathbf{e}_1, \mathbf{e}_2, \mathbf{e}_3, \ldots$ *are errors,* $\mathbf{B_0}', \mathbf{e}'_1, \mathbf{e}'_2, \mathbf{e}'_3, \ldots$ *are tensors produced by Tucker factorization.*

When a BRDF data set is approximated by using our proposed approach, the corresponding *CR* will be:

$$CR = \frac{L(1 + N_{\theta_h} + N_{\phi_h} + N_{\theta_o} + N_{\phi_o})}{N_{\theta_h} N_{\phi_h} N_{\theta_o} N_{\phi_o}}. \tag{9}$$

For a special case when $N_{\theta_h} = N_{\phi_h} = N_{\theta_o} = N_{\phi_o} = N$ then the corresponding *CR* becomes $L(1 + 4N)/N^4$.

To render a colour image at a given outgoing direction, we applied the Tucker approximation to the mean values of measured BRDFs of the three colour channels. Following a similar approach that was used by Ngan et al. [NDM05], we estimated the diffuse and specular parameters for each pair of measured BRDF of each colour channel and the approximated BRDF values using a robust linear regression procedure [DO89].

5. Importance Sampling

The BRDF data can be viewed as sampled frequencies of a multi-variate probability distribution [ÖKB10]. If an empirical estimate of the corresponding probability distribution can be obtained through an appropriate normalization then standard statistical methods can be used to generate incident vectors for a given outgoing direction.

In Figure 3, we illustrate the decomposed univariate Tucker factors of three isotropic materials (*fruitwood-241*, *nickel* and *red-metallic-paint*) and an anisotropic material (*brushed-aluminum*). It is interesting to observe in this figure that the functions of ϕ_h and ϕ_o are approximately uniform for isotropic materials (*fruitwood-241*, *nickel* and *red-metallic-paint*). This suggests that most of the total variation is explained by two components corresponding to

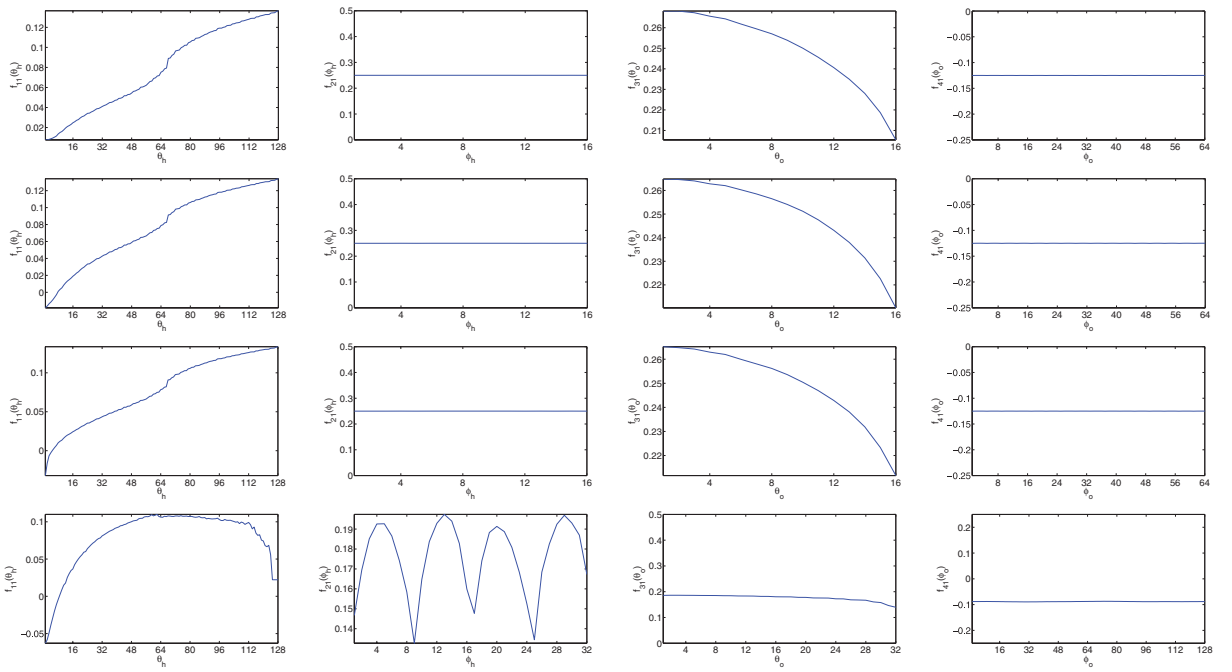

Figure 3: *Plots of Tucker univariate factors for isotropic and anisotropic materials. First row: fruitwood-241 (isotropic), second row: nickel (isotropic) and third row: red-metallic-paint (isotropic). Fourth row brushed-aluminum material (anisotropic).*

univariate functions of θ_h and θ_o. This empirical property has been the case for all of the other isotropic materials considered in this work. We could not establish a physical correspondence for this situation. However, we used this empirical property of the measured data of isotropic materials to facilitate an importance sampling procedure. As may be seen from the figure, a similar property is observed for the anisotropic material also but the univariate factors are the functions of θ_h and ϕ_h for this case.

Based on the empirical properties explained, the Tucker factorization can be used to reduce the 4D sampling problem into a 2D case. Thus, our importance sampling strategy is based on treating the 4D BRDF data as sampled frequencies of the underlying distribution and approximating it by 2D functions.

We define the joint pdf $p_h(\theta_h, \phi_h, \theta_o, \phi_o)$ by normalizing the approximated BRDF $\rho(\theta_h, \phi_h, \theta_o, \phi_o)$ as

$$p_h(\theta_h, \phi_h, \theta_o, \phi_o) = \frac{\rho(\theta_h, \phi_h, \theta_o, \phi_o)\sin\theta_h}{K}, \qquad (10)$$

where

$$K = \sum_{i=1}^{N_{\theta_h}} \sum_{j=1}^{N_{\phi_h}} \sum_{k=1}^{N_{\theta_o}} \sum_{l=1}^{N_{\phi_o}} \rho\left(\theta_h^i, \phi_h^j, \theta_o^k, \phi_o^l\right) \sin\theta_h^i \Delta\theta_h \Delta\phi_h \Delta\theta_o \Delta\phi_o \qquad (11)$$

is the normalizing coefficient, $\Delta\theta_h = \pi/(2N_{\theta_h})$, $\Delta\phi_h = 2\pi/N_{\phi_h}$, $\Delta\theta_o = \pi/(2N_{\theta_o})$ and $\Delta\phi_o = 2\pi/N_{\phi_o}$.

Given an outgoing vector, the incident vector can be generated from the conditional distribution

$$p_h(\theta_h, \phi_h \mid \theta_o, \phi_o) = \frac{p_h(\theta_h, \phi_h, \theta_o, \phi_o)}{K'}, \qquad (12)$$

where

$$K' = \sum_{i=1}^{N_{\theta_h}} \sum_{j=1}^{N_{\phi_h}} p_h(\theta_h^i, \phi_h^j, \theta_o, \phi_o)\Delta\theta_h \Delta\phi_h. \qquad (13)$$

Eq. (1) is defined as a function of $\vec{\omega}_i$ and $\vec{\omega}_o$ over the hemisphere where coordinate system is defined in terms of θ_i, ϕ_i, θ_o and ϕ_o. To convert the halfway representation into this coordinate system we multiply the conditional distribution in Eq. (12) by the Jacobian of the corresponding transformation [PH04] which yields

$$p_i(\vec{\omega}_i \mid \vec{\omega}_o) = \frac{p_h(\theta_h, \phi_h \mid \theta_o, \phi_o)}{4(\vec{\omega}_h \cdot \vec{\omega}_i)}. \qquad (14)$$

5.1. Importance sampling for isotropic materials

We applied Tucker factorization on the logarithms of measured BRDF values, with parameters $n_{\theta_h} = 200$, $n_{\theta_o} = 32$, $n_{\phi_h} = 1$ and $n_{\phi_o} = 1$ on a sample with $N_{\theta_h} \times N_{\phi_h} \times N_{\theta_o} \times N_{\phi_o} = 200 \times 3 \times 32 \times 3$ to obtain a compact representation of BRDF data. Using this representation we

proceeded to perform an importance sampling in a region defined by θ_h and θ_o only since the Tucker factors related to ϕ_h and ϕ_o are approximately constant functions of these parameters.

Based on these considerations, the conditional distribution of θ_h and ϕ_h given that θ_o and ϕ_o can be simplified is

$$p_h(\theta_h, \phi_h \mid \theta_o, \phi_o) = p_h(\theta_h \mid \theta_o). \tag{15}$$

The empirical cdf evaluated at $\theta_h = \theta_h^j$ can be expressed as

$$P_h\left(\theta_h^j \mid \theta_o\right) = \sum_{i=1}^{j} p_h\left(\theta_h^i \mid \theta_o\right)\Delta\theta_h. \tag{16}$$

To simulate the vector $\vec{\omega}_h = (\theta_h, \phi_h)$, first we generate a pair of uniformly distributed random variables (ξ_1 and ξ_2) on the interval [0, 1]. Next ϕ_h is generated as

$$\phi_h = 2\pi\xi_1, \tag{17}$$

and θ_h is generated using the inverse of the empirical cdf P_h in Eq. (16) as

$$\theta_h = P_h^{-1}(\xi_2 \mid \theta_o). \tag{18}$$

θ_h and ϕ_h are substituted in Eq. (14) to evaluate the function value of the conditional pdf. Finally we compute the incident vector using the well-known relationship between the halfway vector and the incident and outgoing direction vectors:

$$\vec{\omega}_i = 2(\vec{\omega}_o \cdot \vec{\omega}_h)\vec{\omega}_h - \vec{\omega}_o. \tag{19}$$

5.2. Importance sampling for anisotropic materials

Importance sampling is performed in a similar way for anisotropic materials as in the isotropic case. For this purpose we used a different anisotropic data set obtained by Ngan et al. [NDM05] who have proposed a method for using their data for direct rendering. We also employed their technique to create anisotropic data. Based on this anisotropic data, we observed that the BRDF depends on θ_h and ϕ_h only as shown in Figure 3 (bottom row). For this data set we used a Tucker factorization with parameters $n_{\theta_h} = 96$, $n_{\phi_h} = 48$, $n_{\theta_o} = 1$ and $n_{\phi_o} = 1$ on a sample with a resolution of $N_{\theta_h} \times N_{\phi_h} \times N_{\theta_o} \times N_{\phi_o} = 256 \times 48 \times 16 \times 16$ for representing the BRDF. The incident vectors are generated using the joint conditional distribution of θ_h and ϕ_h for given values of θ_o and ϕ_o.

Based on the empirical results for the anisotropic BRDFs in Figure 3, marginal distributions of θ_o and ϕ_o can be assumed to be approximately uniform. The conditional distribution of θ_h and ϕ_h given that θ_o and ϕ_o can be written as

$$p_h(\theta_h, \phi_h \mid \theta_o, \phi_o) = p_h(\theta_h, \phi_h). \tag{20}$$

The empirical cdf of ϕ_h can be approximated by

$$P_h\left(\phi_h^j\right) = \sum_{i=1}^{j}\sum_{k=1}^{N_{\theta_h}} p_h\left(\theta_h^k, \phi_h^i\right)\Delta\theta_h\Delta\phi_h. \tag{21}$$

To simulate the vector $\vec{\omega}_h = (\theta_h, \phi_h)$, first we generate ϕ_h as

$$\phi_h = P_h^{-1}(\xi_1), \tag{22}$$

where ξ_1 is a uniform random variable. Then, θ_h is generated using the inverse of the empirical conditional cdf $P_h(\theta_h|\phi_h)$, which is approximated as

$$P_h\left(\theta_h^i \mid \phi_h^j\right) = \sum_{m=1}^{i} \frac{p_h\left(\theta_h^m, \phi_h^j\right)}{\sum_{k=1}^{N_{\theta_h}} p_h\left(\theta_h^k, \phi_h^j\right)}. \tag{23}$$

Finally, for a given ϕ_h and ξ_2, which is a uniform random variable, θ_h is sampled as

$$\theta_h = P_h^{-1}(\xi_2 \mid \phi_h). \tag{24}$$

6. Results

To investigate some empirical properties of the proposed factored model, a data set based on 100 isotropic materials acquired by Matusik et al. [MPBM03] (from the MERL MIT database), and another data set based on four anisotropic materials acquired by Ngan et al. [NDM05] have been used.

As was reported recently, Matusik et al.'s [MPBM03] data include some noisy measurements [LRR04, NDM05]. To minimize sampling errors, we ignored the measurements with incident or outgoing angles greater than 85°. Furthermore, Matusik et al.'s data's missing measurements were estimated by their corresponding column and row averages.

We used samples with a fixed resolution of $N_{\theta_h} \times N_{\phi_h} \times N_{\theta_o} \times N_{\phi_o} = 128 \times 16 \times 16 \times 64$ and $128 \times 32 \times 32 \times 128$ for all isotropic and anisotropic BRDFs, respectively. Samples of resolutions $N_{\theta_h} \times N_{\theta_o} = 200 \times 32$ and $N_{\theta_h} \times N_{\phi_h} = 256 \times 48$ for isotropic and anisotropic importance sampling were also considered.

In this work we used N-way Toolbox [AB00] with the *orthogonal projection* option for all computations corresponding to Tucker factorizations, and ROBUSTFIT [DO89] with the *bisquare* option for estimating the diffuse and specular colour parameters in MATLAB. The rendered images were produced with Physically Based Rendering Toolkit (PBRT) [PH04]. Analytical BRDF models that were chosen for empirical comparisons were fitted to measured BRDF data using Ngan et al.'s fitting procedure [NDM05]. As was suggested by various authors [NDM05, EBJ*06], we considered multiple specular lobes for these analytical models. We

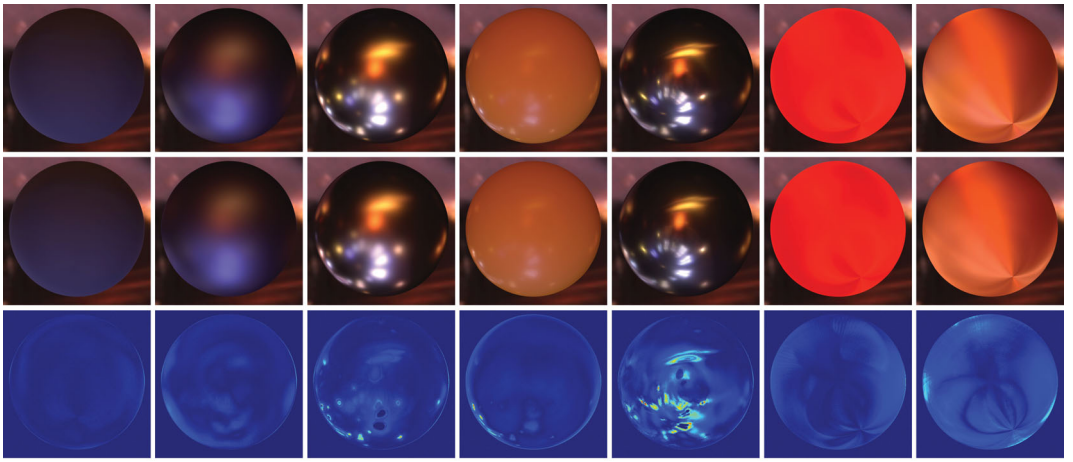

Figure 4: *Spheres were rendered using measured BRDF data and our factored BRDF model: (a) blue-fabric, (b) blue-metallic-paint, (c) nickel, (d) yellow-matte-plastic, (e) grease-covered-steel, (f) red-velvet and (g) yellow-satin materials were presented. All images were rendered at 1024 samples/pixel. Top row: reference images; middle row: our factored model; bottom row: colour-coded differences between the reference images and the rendered images of factored model. For better comparison, colour-coded differences were scaled. Below each image we also report the PSNR value.*

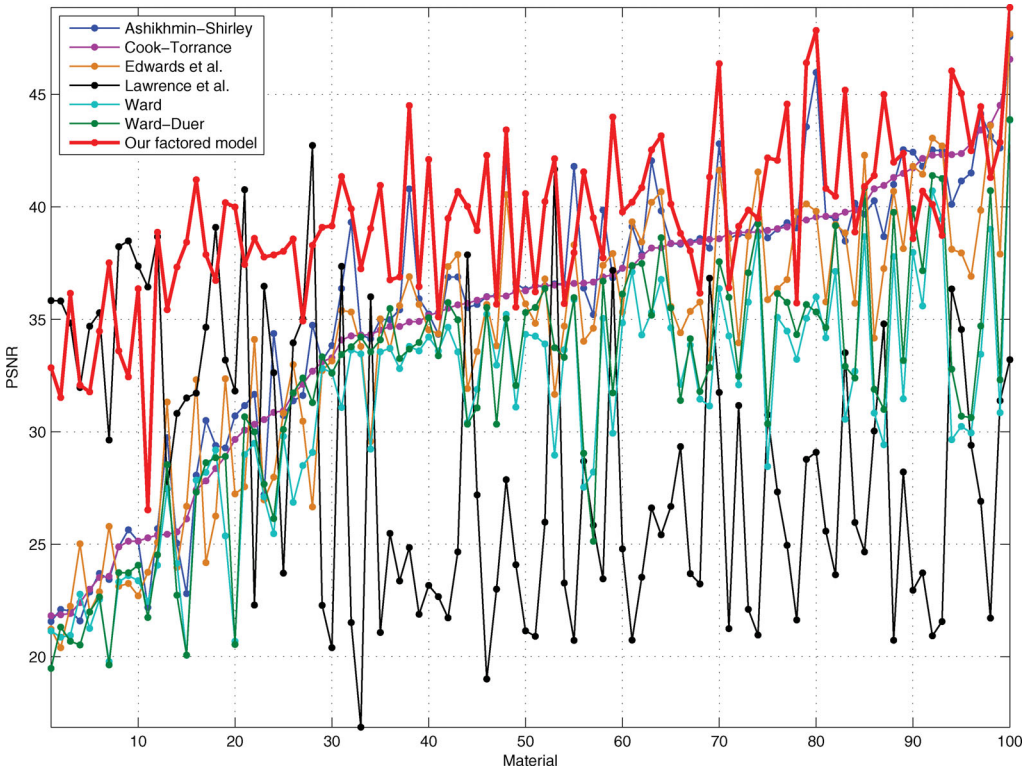

Figure 5: *The PSNR values of seven BRDF models for 100 isotropic materials. The PSNR values are sorted in the PSNRs of the Cook–Torrance model (Magenta) for visualization purpose. Our model gives the highest PSNR values in 66 out of 100 materials (higher is better).*

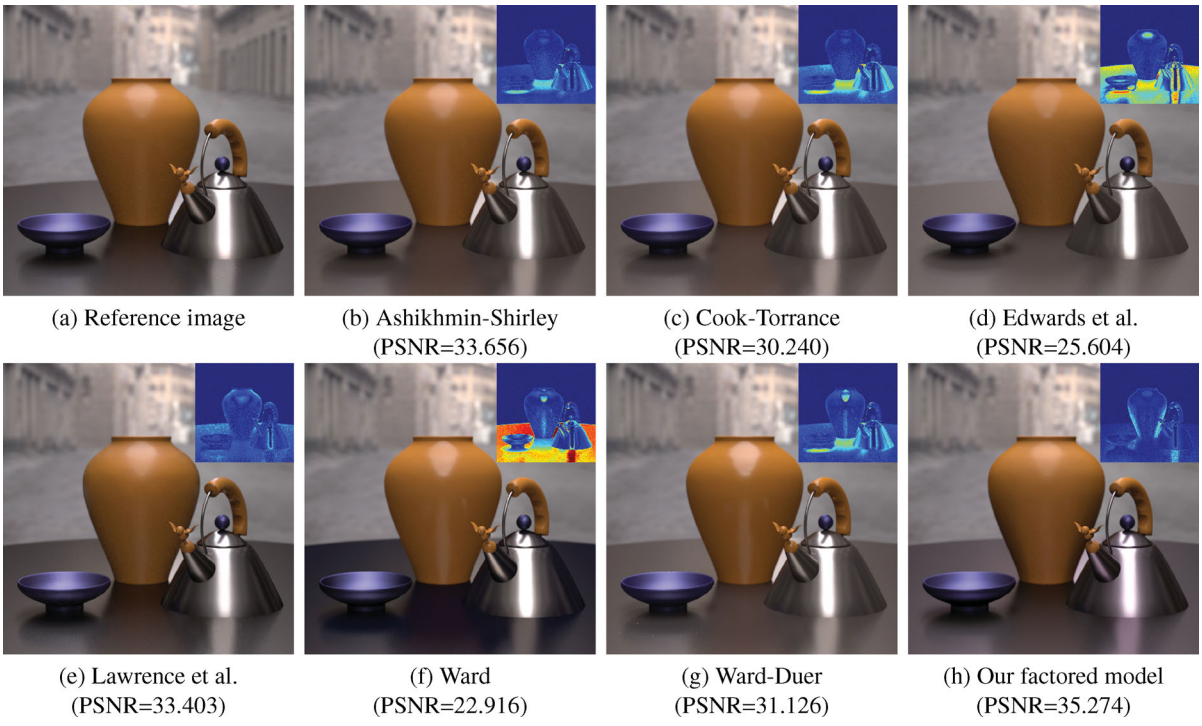

Figure 6: *The Princeton scene was rendered for visual comparisons of well-known BRDF representations. (a) Reference image was rendered using measured BRDF data; (b), (c), (d), (e), (f), (g) and (h) were rendered using the Ashikhmin–Shirley, the Cook–Torrance, the Edwards et al., the Lawrence et al., the Ward, the Ward-Duer and our factored BRDF models, respectively. All images were rendered at 262 144 samples/pixel using a path tracing algorithm. Insets show a colour-coded difference between the reference image and the rendered image. For better comparison, colour-coded differences were scaled. Below each image we also report the PSNR value.*

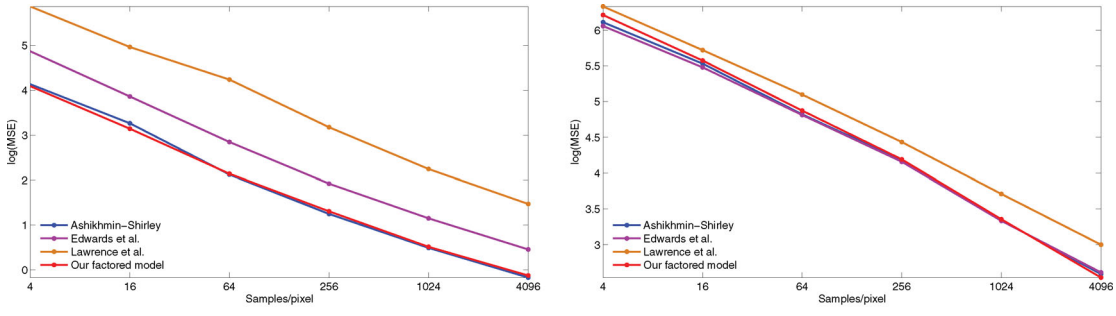

Figure 7: *(a) Image MSE for measured nickel BRDF as a function of the number of samples in constant environment. (b) Image MSE for measured nickel BRDF as a function of the number of samples in Grace Cathedral environment. At 256 paths/pixel we see the values for which the factor of improvement is listed in Tables 1 and 2.*

compared our rendering results with those of Lawrence et al. [LRR04], using the parameter values given in their paper. The peak signal-to-noise ratio (PSNR) [Ric02] values were obtained to compare the visual quality of the underlying models.

Based on our model, renderings under direct illumination are shown in Figure 4 for various isotropic and anisotropic materials. It can be seen from the colour-coded difference images that our compact factored model provides a satisfactory representation both for isotropic and for anisotropic

materials. Using 100 isotropic materials, we carried out an extensive comparison of our model with six well-known BRDF models, namely Ashikhmin–Shirley [AS00], Cook–Torrance [CT81], Edwards et al. [EBJ*06], Lawrence et al. [LRR04], Ward [War92] and Ward-Duer [Due05] (Figure 5). It is interesting to observe that the proposed model has resulted in the highest PSNR values in 66 cases and performed well for the remaining 34 materials. We also obtained renderings of the Princeton scene [LRR04, EBJ*06] and presented these in Figure 6. The PSNR values calculated for the materials given in the figure shows that our factored BRDF model gives the best representation for this special case.

We notice that the BRDF properties at grazing angles are represented well with our method. However, for specular regions appear to be more specular than expected for highly specular materials such as brass, chrome, chrome-steel and red-metallic-paint (see supplementary document).

To evaluate the efficiency of our importance sampling procedure quantitatively, we rendered spheres (visibility is not considered) lit by both constant and complex environment maps. The importance sampling methods selected for comparison include analytical samplings of Ashikhmin–Shirley [AS00], Edwards et al. [EBJ*06] BRDF models and Lawrence et al.'s [LRR04] factored BRDF model.

To investigate the effects of importance sampling procedures on the image quality, we calculated the MSEs for various sample sizes (number of samples per pixel). The mean squared errors (MSEs) obtained for blue-metallic-paint, nickel and yellow-matte-plastic are shown in Figure 7. Reference images used in these comparisons were rendered with 262 144 samples per pixel. We also compared our method with the others in terms of the ratios of corresponding MSEs. The results for constant and complex environments are given in Tables 1 and 2, respectively. The ratios of the MSEs given in these tables can be used to estimate about how much longer the alternative approaches would need to run to produce the same quality results in rendered images as our method. Ratios greater than 1 indicate that the proposed importance sampling procedure performs better than its competitors. As is seen from Figure 7 and Tables 1 and 2, our importance sampling method gives comparable results. We also rendered the Princeton scene using a path tracer with global illumination, which is shown in Figure 8. In this case, multiple importance sampling (MIS) methods [VG95] do not work, therefore the BRDF sampling is the only reasonable strategy. In Figure 8, it should be noted that the differences in the glossy highlights are caused by different approximations produced by the respective models (e.g. our representation cause colour-shift); the importance sampling itself is unbiased. Clearly, our importance sampling method is comparable to the importance sampling technique presented by Ashikhmin–Shirley [AS00] and Lawrence et al. [LRR04]. The sampling times based on 256 samples per pixel for the Princeton scene which was rendered under direct illumination, were found to be 1067.392, 1109.015, 1161.327 and 1261.461 seconds for Lawrence et al. [LRR04], Ashikhmin–Shirley [AS00], our Tucker importance sampling procedure and Edwards et al. [EBJ*06], respectively. These results show that sampling times are approximately the same for all importance sampling algorithms.

Table 1: *The efficiency of BRDF sampling in a constant environment. This table lists the factor of improvement in MSEs resulting from sampling the BRDF according to our factored representation in the constant environment.*

Material	Blue-metallic-paint	Nickel	Yellow-matte-plastic
Ashikhmin–Shirley	0.5697	0.9432	0.7328
Edwards et al.	0.5330	1.8501	0.8134
Lawrence et al.	0.4099	6.4845	1.3159

Table 2: *The efficiency of BRDF sampling in Grace Cathedral environment. This table lists the factor of improvement in MSEs resulting from sampling the BRDF according to our factored representation in the Grace Cathedral environment.*

Material	Blue-metallic-paint	Nickel	Yellow-matte-plastic
Ashikhmin–Shirley	1.029	0.9903	0.9361
Edwards et al.	0.8851	0.9672	0.9111
Lawrence et al.	1.0158	1.2752	1.0759

We also compared the storage need of our model with another factored BRDF model proposed by Lawrence et al. [LRR04]. As it can be seen from Table 3, the storage needs of our factored BRDF model are roughly two–three times less than that of Lawrence et al.'s representation, while providing better representation. The parameter L defined in Eq. (9) plays an important role both for storage complexity and representation ability. The values for L used in this comparison are 15, 15 and 13 for blue-metallic-paint, nickel and yellow-matte-plastic, respectively. Our empirical results have shown that a typical number of iterations (L) is about 13.

A similar comparison was performed on rendering times of the models based on Figure 4. The corresponding results are presented in Table 4. Rendering times were acquired on an Intel Core i7 2.66 GHz computer with a 12 GB memory. As seen from Table 4 that the rendering times of our factored BRDF model is slightly higher than the rendering times of the other models.

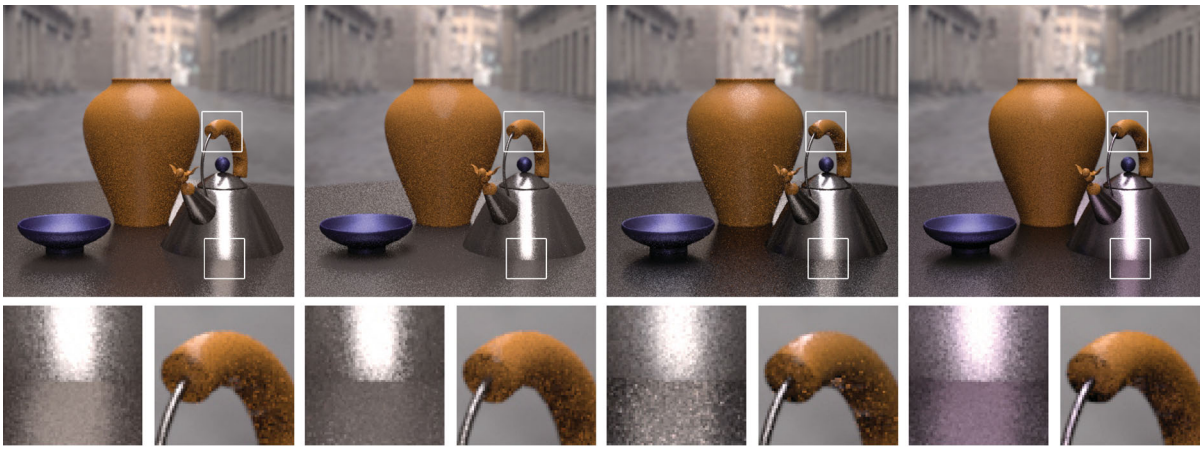

(a) Ashikhmin-Shirley sampling (b) Edwards et al. sampling (c) Lawrence et al. sampling (d) Our factored sampling

Figure 8: *For visual comparison of sampling efficiency, the Princeton scene was rendered using a path tracer for global illumination and paths up to five bounces were included: (a), (b), (c) and (d) were rendered using the Ashikhmin–Shirley BRDF, the Edwards et al. BRDF, the Lawrence et al.'s factored BRDF and our factored BRDF at 256 samples/pixel, respectively. The bottom row shows closeups of highlighted regions for all models.*

Table 3: *Required storage spaces by the three BRDF representations for various materials. Rendering data are prepared in binary double precision for all BRDF representations.*

BRDF Model	Blue-metallic-paint	Nickel	Yellow-matte-plastic
Measured	33.4 MB	33.4 MB	33.4 MB
Lawrence et al.	139.0 KB	96.5 KB	331.9 KB
Our factored model	76.7 KB	76.7 KB	73.2 KB

Table 4: *Rendering times (in seconds) of various BRDF representations.*

BRDF Model	Blue-metallic-paint	Nickel	Yellow-matte-plastic
Measured	1802.83	1894.33	1830.87
Cook–Torrance	1647.43	1759.23	1770.70
Lawrence et al.	1854.53	1795.97	1831.27
Ward	1465.93	1563.70	1591.10
Our factored model	2048.73	2122.40	2015.23

7. Conclusions and Future Work

In this paper, we have introduced a factored BRDF model which provided good approximation and an efficient importance sampling for BRDF. Our factored BRDF representation can be considered as a compression technique for measured BRDF data. We showed that our factored method can provide good approximations both for isotropic and anisotropic materials. Furthermore, we showed that our importance sampling procedure performed as well as other well-known importance sampling techniques.

Our future work will be continued to generalize the proposed factorization technique to higher dimensional data and to implement our factored BRDF representation in real-time global illumination algorithms.

Appendix

Algorithm 1 performs logarithmic transformation on the measured BRDF data.

Algorithm 2 calculates the coefficients of Tucker factors for a given number of iterations (L) by using the factorization algorithm (*tuckerFit*) [AB00]. This algorithm also employs *robustFit* [DO89] to obtain the robust regression estimates of diffuse and specular parameters. While *tuckerFit* function uses *orthogonal projection* option as a default parameter, *robustFit* function uses *bisquare* option as a default parameter.

Algorithm 3 reconstructs a tensor using the coefficients of Tucker factors. Finally, Algorithm 4 evaluates the estimated BRDF values.

Algorithm 1: prepareFittingData(measuredBRDF)

1: /*$\mathbf{B}_r$, $\mathbf{B}_g$ and $\mathbf{B}_b$ are BRDF tensors for each color channel*/
2: $\mathbf{B} = (\mathbf{B}_r + \mathbf{B}_g + \mathbf{B}_b)/3$
3: $\mathbf{B}_0 = \log(\mathbf{B})$
4: return $\mathbf{B}_0$

Algorithm 2: fittingProcedure($\mathbf{B}_0$, L)

1: let $\mathbf{e} = \mathbf{B}_0$
2: let **logBRDF** $= 0$
3: for $i = 1$ to L
4: $[g_i, f_{1\{i\}}, f_{2\{i\}}, f_{3\{i\}}, f_{4\{i\}}] = tuckerFit(\mathbf{e})$
5: $\mathbf{e} = \mathbf{e} - tuckerEvaluateTensor(g_i, f_{1\{i\}}, f_{2\{i\}}, f_{3\{i\}}, f_{4\{i\}})$
6: end for
7: for $i = 1$ to L
8: **logBRDF** $=$ **logBRDF**$+$ $tuckerEvaluateTensor(g_i, f_{1\{i\}}, f_{2\{i\}}, f_{3\{i\}}, f_{4\{i\}})$
9: end for
10: $[k_{dr}, k_{sr}] = robustFit(\exp(\mathbf{logBRDF}), \mathbf{B}_r)$
11: $[k_{dg}, k_{sg}] = robustFit(\exp(\mathbf{logBRDF}), \mathbf{B}_g)$
12: $[k_{db}, k_{sb}] = robustFit(\exp(\mathbf{logBRDF}), \mathbf{B}_b)$
13: return $g_{\{1...L\}}, f_{1\{1...L\}}, f_{2\{1...L\}}, f_{3\{1...L\}}, f_{4\{1...L\}}, k_{dr}, k_{dg}, k_{db}, k_{sr}, k_{sg}, k_{sb}, k_{sr}, k_{sg}, k_{sb}$

Algorithm 3: tuckerEvaluateTensor(g, f_1, f_2, f_3, f_4)

1: let **evaluatedTensor** $= 0$
2: for $i = 1$ to N_{θ_h}
3: for $j = 1$ to N_{ϕ_h}
4: for $k = 1$ to N_{θ_o}
5: for $l = 1$ to N_{ϕ_o}
6: **evaluatedTensor**$_{ijkl} = g * f_1(i) * f_2(j) * f_3(k) * f_4(l)$
7: end for
8: end for
9: end for
10: end for
11: return **evaluatedTensor**

Algorithm 4: renderTuckerBrdf($g_{\{1...L\}}, f_{1\{1...L\}}, f_{2\{1...L\}}, f_{3\{1...L\}}, f_{4\{1...L\}}, \theta_{hind}, \phi_{hind}, \theta_{oind}, \phi_{oind}, k_{dr}, k_{dg}, k_{db}, k_{sr}, k_{sg}, k_{sb}$)

1: let **logBRDF** $= 0$
2: for $i = 1$ to L
3: **logBRDF** $=$ **logBRDF** $+ g_{1\{i\}} * f_{1\{i\}}(\theta_{hind}) * f_{2\{i\}}(\phi_{hind}) * f_{3\{i\}}(\theta_{oind}) * f_{4\{i\}}(\phi_{oind})$
4: end for
5: return $k_{dr} + k_{sr} * \exp(\mathbf{logBRDF}), k_{dg} + k_{sg} * \exp(\mathbf{logBRDF}), k_{db} + k_{sb} * \exp(\mathbf{logBRDF})$

Acknowledgments

The authors thank anonymous reviewers for their comments and Wojciech Matusik et al. [MPBM03] for using their measured BRDF data. This work was supported by a grant from the Scientific and Technical Research Council of Turkey (Project No:108E007).

References

[AB00] Andersson C. A., Bro R.: The n-way toolbox for matlab. *Chemometrics and Intelligent Laboratory Systems 52*, 1 (Aug. 2000), 1–4.

[AS00] Ashikhmin M., Shirley P.: An anisotropic Phong BRDF model. *Journal of Graphics Tools*, 5, 2 (2000), 25–32.

[Bli77] Blinn J. F.: Models of light reflection for computer synthesized pictures. *Computer Graphics 11*, 2 (1977), 192–198. (Proc. SIGGRAPH '77).

[CT81] Cook R. L., Torrance K. E.: A reflectance model for computer graphics. *Computer Graphics 15*, 3 (1981), 307–316. (Proc. SIGGRAPH '81).

[DO89] Dumouchel W. H., O'brien F. L.: Integrating a robust option into a multiple regression computing environment. In *Computing Science and Statistics: Proceedings of the 21st Symposium on the Interface* (Alexandria, VA, 1989), K. Berk and L. Malone (Eds.). American Statistical Association, pp. 297–301.

[Due05] Duer A.: On the Ward model for global illumination. Unpublished material, 2005.

[EBJ*06] Edwards D., Boulos S., Johnson J., Shirley P., Ashikhmin M., Stark M., Wyman C.: The halfway vector disk for BRDF modeling. *ACM TOG 25*, 1 (Jan. 2006), 1–18.

[Hit27a] Hitchcock F. L.: The expression of a tensor or a polyadic as a sum of products. *Journal of Mathematics and Physics*, *6*, 1 (1927), 164–189.

[Hit27b] Hitchcock F. L.: Multiple invariants and generalized rank of a p-way matrix or tensor. *Journal of Mathematics and Physics*, *7*, 1 (1927), 39–79.

[HTSG91] He X. D., Torrance K. E., Sillion F. X., Greenberg D. P.: A comprehensive physical model for light reflection. *Computer Graphics 25*, 4 (1991), 175–186. (Proc. SIGGRAPH '91).

[Kaj85] Kajiya J. T.: Anisotropic reflection models. *Computer Graphics 19*, 3 (1985), 15–21. (Proc. SIGGRAPH '85).

[Kaj86] Kajiya J. T.: The rendering equation. *Computer Graphics 20*, 4 (1986), 143–150. (Proc. SIGGRAPH '86).

[KB09] Kolda T. G., Bader B. W.: Tensor decompositions and applications. *SIAM Review 51*, 3 (Sept. 2009), 455–500.

[KM99] Kautz J., Mccool M. D.: Interactive rendering with arbitrary BRDFs using separable approximations. In *Proceedings of Eurographics Workshop on Rendering* (Granada, Spain, 1999), D. Lischinski and G. W. Larson (Eds.). Eurographics Association, pp. 247–260.

[KvDS96] Koenderink J. J., van Doorn A. J., Stavridi M.: Bidirectional reflection distribution function expressed in terms of surface scattering modes. In *ECCV '96: Proceedings of the 4th European Conference on Computer Vision-Volume II* (London, UK, 1996), B. F. Buxton and R. Cipolla (Eds.), vol. 1065 of *Lecture Notes in Computer Science*, Springer-Verlag, pp. 28–39.

[LF97] Lalonde P., Fournier A.: A wavelet representation of reflectance functions. *IEEE Transactions on Visualization and Computer Graphics*, 3, 4 (1997), 329–336.

[LFTG97] Lafortune E. P., Foo S.-C., Torrance K. E., Greenberg D. P.: Non-linear approximation of reflectance functions. In *Proceedings SIGGRAPH '97* (New York, NY, USA, 1997), ACM Press/Addison-Wesley Publishing Co., pp. 117–126.

[LRR04] Lawrence J., Rusinkiewicz S., Ramamoorthi R.: Efficient BRDF importance sampling using a factored representation. *ACM TOG 23*, 3 (2004), 496–505. (Proc. SIGGRAPH '04).

[LRR05] Lawrence J., Rusinkiewicz S., Ramamoorthi R.: Adaptive numerical cumulative distribution functions for efficient importance sampling. In *Proceedings of Eurographics Symposium on Rendering* (Konstanz, Germany, 2005), K. Bala and P. Dutré (Eds.), Eurographics Association, pp. 11–20.

[MAA01] Mccool M. D., Ang J., Ahmad A.: Homomorphic factorization of BRDFs for high-performance rendering. In *Proceedings SIGGRAPH '01* (New York, NY, USA, 2001), ACM, pp. 171–178.

[MPBM03] Matusik W., Pfister H., Brand M., Mcmillan L.: A data-driven reflectance model. *ACM TOG 22*, 3 (July 2003), 759–769. (Proc. SIGGRAPH '03).

[MUGL08] Montes R., Ureña C., García R. J., Lastra M.: Generic BRDF sampling: A sampling method for global illumination. In *Proceedings of Third International Conference on Computer Graphics Theory and Applications* (Funchal, Madeira, Portugal, 2008), J. Braz, N. J. Nunes and J. M. Pereira (Eds.), pp. 191–198.

[NDM05] Ngan A., Durand F., Matusik W.: Experimental analysis of BRDF models. In *Proceedings of Eurographics Symposium on Rendering* (Konstanz, Germany, 2005), K. Bala and P. Dutré (Eds.), Eurographics Association, pp. 117–126.

[NNSK99] Neumann L., Neumann A., Szirmay-Kalos L.: Compact metallic reflectance models. *Computer Graphics Forum*, *18*, 3 (1999), 161–172.

[ÖKB10] Öztürk A., Kurt M., Bilgili A.: A copula based BRDF model. *Computer Graphics Forum 29*, 6 (Sept. 2010), 1795–1806.

[OKBG08] Ozturk A., Kurt M., Bilgili A., Gungor C.: Linear approximation of bidirectional reflectance distribution functions. *Computers & Graphics 32*, 2 (April 2008), 149–158.

[ON94] Oren M., Nayar S. K.: Generalization of Lambert's reflectance model. In *Proceedings SIGGRAPH '94* (New York, NY, USA, 1994), ACM, pp. 239–246.

[PF90] Poulin P., Fournier A.: A model for anisotropic reflection. *Computer Graphics 24*, 4 (1990), 273–282. (Proc. SIGGRAPH '90).

[PH04] Pharr M., Humphreys G.: *Physically Based Rendering: From Theory to Implementation*. Morgan Kaufmann Publishers Inc., San Francisco, CA, 2004.

[Pho75] Phong B. T.: Illumination for computer generated pictures. *Commun. ACM 18*, 6 (June 1975), 311–317.

[Ric02] Richardson I. E.: *Video Codec Design: Developing Image and Video Compression Systems*. John Wiley & Sons, Inc., New York, NY, 2002.

[Rus98] Rusinkiewicz S. M.: A new change of variables for efficient BRDF representation. In *Proceedings of Eurographics Workshop on Rendering* (Vienna, Austria, 1998), G. Drettakis and N. L. Max (Eds.), Springer, pp. 11–22.

[RVZ08] Romeiro F., Vasilyev Y., Zickler T.: Passive reflectometry. In *ECCV '08: Proc. of the 10th European Conference on Computer Vision: Part IV* (Marseille, France, 2008), D. A. Forsyth, P. H. S. Torr and A. Zisserman (Eds.), vol. 5305 of *Lecture Notes in Computer Science*, Springer-Verlag, pp. 859–872.

[SAS05] Stark M. M., Arvo J., Smits B.: Barycentric parameterizations for isotropic BRDFs. *IEEE Transactions on Visualization and Computer Graphics 11*, 2 (March 2005), 126–138.

[SS95] Schröder P., Sweldens W.: Spherical wavelets: Efficiently representing functions on the sphere. In *Proc. SIGGRAPH '95* (New York, NY, USA, 1995), ACM, pp. 161–172.

[SZC*07] Sun X., Zhou K., Chen Y., Lin S., Shi J., Guo B.: Interactive relighting with dynamic BRDFs. *ACM TOG 26*, 3 (2007), 27:1–27:10. (Proc. SIGGRAPH '07).

[TS67] Torrance K. E., Sparrow E. M.: Theory for off-specular reflection from roughened surfaces. *Journal of the Optical Society of America 57*, 9 (Sept. 1967), 1105–1114.

[Tuc63] Tucker L. R.: Implications of factor analysis of three-way matrices for measurement of change. In *Problems in Measuring Change*, C. W. Harris (Ed.), University of Wisconsin Press, Madison, WI, 1963, pp. 122–137.

[Tuc64] Tucker L. R.: The extension of factor analysis to three-dimensional matrices. In *Contributions to Mathematical Psychology*, H. Gulliksen and N. Frederiksen (Eds.), Holt, Rinehart and Winston, New York, 1964, pp. 110–127.

[Tuc66] Tucker L. R.: Some mathematical notes on three-mode factor analysis. *Psychometrika 31*, 3 (Sept. 1966), 279–311.

[VG95] Veach E., Guibas L. J.: Optimally combining sampling techniques for Monte Carlo rendering. In *Proc. SIGGRAPH '95* (New York, NY, USA, 1995), ACM, pp. 419–428.

[VT04] Vasilescu M. A. O., Terzopoulos D.: Tensortextures: Multilinear image-based rendering. *ACM TOG 23*, 3 (2004), 336–342. (Proc. SIGGRAPH '04).

[War92] Ward G. J.: Measuring and modeling anisotropic reflection. *Computer Graphics 26*, 2 (1992), 265–272. (Proc. SIGGRAPH '92).

[WAT92] Westin S. H., Arvo J. R., Torrance K. E.: Predicting reflectance functions from complex surfaces. *Computer Graphics 26*, 2 (1992), 255–264. (Proc. SIGGRAPH '92).

[WWS*05] Wang H., Wu Q., Shi L., Yu Y., Ahuja N.: Out-of-core tensor approximation of multi-dimensional matrices of visual data. *ACM TOG 24*, 3 (2005), 527–535. (Proc. SIGGRAPH '05).